

Steady-State Fluorescence of Dye-Sensitized TiO₂ Xerogels and Aerogels as a Probe for Local Chromophore Aggregation[†]

Annette R. Howells and Marye Anne Fox*

Department of Chemistry, North Carolina State University, Raleigh, North Carolina 27965-8204

Received: August 1, 2002

Sol–gel synthesis has been used to disperse an emissive chromophore within a porous TiO₂ matrix, leading to xerogels and aerogels doped with tethered and unbound pyrenyl groups. Steady-state fluorescence was used to probe the interactions of neighboring pyrene groups within the gel matrix. Changes in the relative intensity of the monomer (*I*₁) emission peak as a function of chromophore concentration indicated a local interaction between included dyes for both tethered and unbound pyrene groups, likely through π stacking. Partial matrix methylation or phenylation failed to produce a significant effect on the relative intensity of the *I*₁ signal in either the xerogel or the aerogel. Changes in the relative intensity of excimer emission with changes in matrix composition, however, do suggest that the presence of either phenyl or methyl groups within the TiO₂ matrix impedes π stacking between pairs of tethered pyrenyl groups. Compared with strong excimer emission in the xerogels containing pyrenyl groups at relatively high concentrations, excimer formation was inhibited in the corresponding aerogels, for which BET analysis indicated a broad pore size distribution in the mesoporous range, ca. 100 Å.

1. Introduction

Nanocrystalline semiconductors have been studied extensively as suspended small particles,^{1–4} powders,^{5–8} and polycrystalline films.^{9–12} In particular, nanocrystalline TiO₂ has received considerable attention because of its high photocatalytic activity, especially in applications for solar energy conversion and in the oxidative degradation of pollutants.^{13–18} Photosensitization of the metal oxide surface by immobilized dyes, such as metalloporphyrins or carboxylated ruthenium polypyridines, gives rise to extended wavelength responsiveness beyond that attained by band gap irradiation.^{19–22} In this application, high surface area supports are preferred because photosensitization efficiency is diminished at surface coverages in excess of one monolayer.^{10, 23}

The successful use of silicate sol–gels as high surface supports for the dispersion of catalysts suggests that similar improvements in dye-sensitized photocatalysis might be achieved if a highly porous titanate gel were employed. If a dye is bound covalently or is physisorbed within such a matrix, the adverse effects of self-quenching should be minimized because single molecules of the dye might be isolated in the condensed titanium oxide matrix.²⁷ This composite would also permit achieving high optical density of the absorptive dye. We are particularly interested therefore in examining how chromophore-loaded titanate sol–gels can affect excited-state properties of included molecules that can act as photosensitizers.

Sol–gel synthetic methods have been used to produce a variety of inorganic and inorganic–organic composite materials with varying morphological properties. The hydrolysis and polycondensation of organic titanates proceed rapidly under mild reaction conditions and at low temperatures, enabling the preparation of single-phase mixtures of metal and semimetal oxides and a uniform dispersal of organic molecules within the

resulting porous inorganic matrix.^{24–30} Although most sol–gels studied so far are silica-based, the same synthetic routes also apply to titania.

Sol solutions can be spin-cast or dip-coated onto solid supports to form thin films or cast as block monolith structures.^{24,25} Powders with monodisperse particle size distributions can also be obtained.²⁵ Sol–gel-derived inorganic oxides are often preferred as supports for immobilized reagent species, because of the relative optical transparency, thermal stability, and molecular permeability of these materials. Reported applications include usage as chemical sensors,³¹ in optoelectronics,^{1,32} and in photonics.^{33–34}

The spectroscopy of dye-modified gels can be used not only as probes to characterize the internal structure of these porous host matrices but also to monitor the influence of the local environment on excited-state properties of the included dye. This technique was first applied to sol–gels by Avnir et al. who monitored the fluorescence emission of an included pyrene throughout sol formation, gelation, and condensation.^{35,36} Two aspects of the excited-state dynamics of pyrene were found to be especially significant with respect to the physical characterization of a sol–gel-derived host matrix.^{35,37–40} First, pyrene forms an excimer that emits at wavelengths significantly longer than those characteristic of an isolated pyrene monomer. Second, the emission signal attributed to pyrene monomer exhibits vibronic structure that is highly sensitive to environmental polarity. Because a metal oxide sol–gel contains a finite number of terminal bonds, hydroxy and alkoxy functional groups are present on the internal surfaces of the metal oxide matrix,^{25,27,37} enhancing local polarity. Thus, the geometric constraints imposed by the nature of the sol, by the swelling of the gel matrix, and by the interactions of included pyrene probes with surface functional groups will impact the observed fluorescent response.

In our current study, TiO₂ block monoliths (xerogels and aerogels) were doped with pyrene derivatives, either covalently

[†] Part of the special issue “George S. Hammond & Michael Kasha Festschrift”.

bound to or trapped without chemical bonds within the matrix. A dye-functionalized titanate (**1**) bearing a 1-pyrenylmethyl group (R-Ti(OCHMe₂)₃; **1**, R = CH₂-Pyr (Pyr is 1-pyrenyl); **2**, R = C₆H₅; **3**, R = CH₃) was copolymerized with tetrakis(isopropoxy)Ti(IV) to produce a functionalized TiO₂ matrix. The introduction of an additional coupling component such as a trichlorosilane or phosphate functional group,^{5,41} reported to stabilize metal oxide matrices, proved to be unnecessary in the synthesis of structurally rigid monoliths. The local chemical environment within the gel matrix could be further altered by including an alkyl or aryl titanate with the monomer sol solution. For this purpose, specially functionalized Ti(IV) monomers (phenylated **2** and methylated **3**) replaced titanium isopropoxide in the copolymerization. Steady-state fluorescence was then used to characterize the excited-state properties of the dye contained within a composite monolith.

2. Experimental Procedure

2.1. Materials. Tetra(isopropyl)orthotitanate, chlorotri(isopropoxy)titanium(IV), and anhydrous hydrazine were reagent grade and used as received from Aldrich. Potassium *tert*-butoxide (Aldrich) was stored in a drybox after opening. *n*-Butyllithium (1.6 M in hexanes, Aldrich), phenyllithium (1.8 M in cyclohexanes/ether 70%/30%, Aldrich), methylolithium (1.4 M ethyl ether, Aldrich), hexane (Fisher), ethylene glycol (Fisher), *n*-amyl acetate (Fisher), anhydrous ethanol (Fisher), pentane (Fisher), pyrene (Aldrich), and 1-pyrenylcarboxaldehyde (Aldrich) were used as received. Anhydrous ethyl ether and tetrahydrofuran purchased in Sure SealTM bottles (Aldrich) were used for Schlenk line procedures.

2.2. Synthesis of (1-Pyrenylmethyl)triisopropoxytitanium, 1. The preparation was adapted from a preparation of (1-pyrenylmethyl)trimethoxysilane.³⁸ Potassium *tert*-butoxide (5.3 mmol) was added to a solution of 5 mmol of 1-methylpyrene in 50 mL of Et₂O under Ar. *n*-Butyllithium (5 mmol) was added slowly, generating a deep burgundy-colored solution. The resulting solution was stirred for 3 h under Ar. Chlorotri(isopropoxy)titanium(IV) (5 mmol) in ethyl ether was added dropwise while stirring over 45 min. The resulting solution, which was cloudy and yellow, was stirred for 10 h and then filtered under Ar. The yellow crystals obtained upon solvent extraction were redissolved in anhydrous ethyl ether (0.01 M) and stored under Ar. Upon long-term storage in moist air, **1** underwent complete hydrolysis, so surface isopropoxy ligands converted to hydroxy groups. The hydrolyzed structure was used in the structural analysis of the doped gels. **1**: ¹H NMR(CDCl₃, 400 MHz) δ 2.99 (2 H, s), 7.86 (1 H, d, *J* = 8.0 Hz), 7.97 (1 H, t, *J* = 8.0 Hz), 8.01 (2 H, m), 8.08 (1 H, m), 8.10 (1 H, d, *J* = 9.2 Hz), 8.15 (1 H, m), 8.17 (1 H, m), 8.24 (1 H, d, *J* = 9.2 Hz); ¹³C NMR (CDCl₃, 400 MHz) δ 31.19, 123.93, 124.90, 124.97, 125.04, 126.00, 126.65, 127.34, 127.77, 128.09, 129.43, 129.95, 131.21, 131.67, 132.48; FAB(+) 314.27 (9), 313.27 (31), 273.28(16), 272.27(34), 217.25 (44), 216.24 (100).

2.3. Synthesis of Phenyltriisopropoxytitanium(IV), 2. The preparation of **2** has been described.⁴² ¹H NMR(CDCl₃, 300 MHz) δ 1.24 (18 H, d, *J* = 6.3 Hz), 4.45 (3 H, sep, *J* = 6.3 Hz), 7.32 (1 H, t, *J* = 7.2 Hz), 7.42 (2 H, t, *J* = 7.5 Hz), 7.58(2 H, d, *J* = 7.8 Hz).

2.4. Synthesis of Methyltriisopropoxytitanium(IV), 3. The preparation of **3** has been described.⁴³ ¹H NMR(CDCl₃, 400 MHz) δ 1.20 (3 H, s), 1.24 (18 H, d, *J* = 6.4 Hz), 4.51 (3 H, sep, *J* = 6.4 Hz); ¹³C NMR (CDCl₃, 400 MHz) δ 25.56, 26.756, 76.42.

2.5. Preparation of Xerogels. The preparation of TiO₂ monolith gels from tetrakis(isopropoxy)titanium(IV) has been

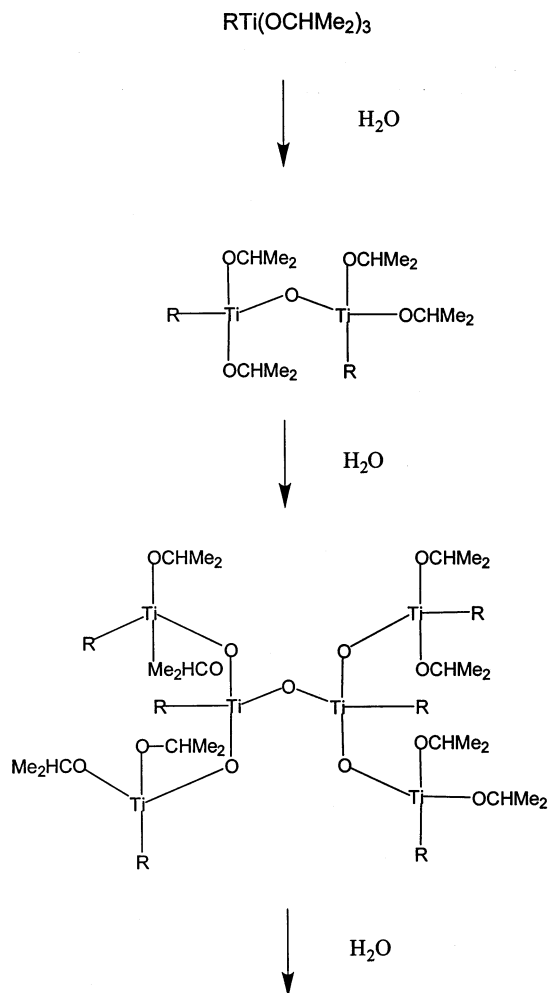
described.^{27,28} HCl, distilled-deionized water, anhydrous ethanol, and tetrakis(isopropoxy)titanium(IV) were mixed in the molar ratio 0.6:0.4:1:0.1, respectively. The Ti(IV) was added to a solution of the remaining reagents while stirring. Gelation occurred within 5–10 min. After 3 min of stirring, 1.9 mL aliquots of the sol solution were dispensed into polystyrene vials, which served as monolith molds. Gels were aged in capped vials for 7 days. After 1 week, the vial caps were removed, drilled with a 3/16 in. drill bit, and replaced on the sample vials. The gels were then stored at room temperature at a relative humidity in excess of 70%, allowing for the gradual evaporation of solvent from the sample vials.

The resulting gels were aged under these conditions for 3–6 weeks. During this period, the gels exhibited massive contraction. The mass of a fully aged gel was approximately 1/10 of the mass of the initial aliquot of the sol solution. This contraction was accomplished by an appreciable weight loss resulting from the evaporation of solvent, water, and 2-propanol formed during condensation. A corresponding reduction in volume was also observed as the gel contracted and solvent was expelled from the porous matrix. Fully formed gels were hard and transparent. The final shape of the gel corresponded to the shape of the polystyrene mold. The use of a round vial as mold allowed for a uniform contraction.

To introduce the absorptive pyrenyl dye, the functionalized monomer **1** was added to the ethanol/water/acid solution prior to the addition of the tetrakis(isopropoxy)Ti(IV) monomer. Concentrations of the dye-functionalized monomer in the sol solution ranged from 10⁻² to 10⁻⁵ M. To attain optical matching, the gels were doped at equivalent concentrations of bound and occluded groups. In the phenyl-functionalized gels, **2** replaced 1% of the Ti(IV) monomer precursor. At higher concentrations, gels turned white and opaque. In the methyl-functionalized gels, concentrations of **3** as large as 5% monomer could be used successfully. Again, at higher concentrations, the methylated gels turned white and opaque over the course of aging.

2.6. Aerogel Preparation. Aerogels were prepared from wet gels, followed by supercritical drying in CO₂.^{28,44,45} With *n*-amyl acetate as an intermediate solvent, the gels were aged in capped vials for 7 days prior to ethanol extraction and supercritical drying. Smaller aliquots of the sol solution were used for the aerogel samples to limit the thickness of the wet gel (<2 mL). As these gels dried, they formed an extremely brittle monolith. Some yellow discoloration, attributable to residual solvent, was usually observed. At low concentrations of the dye-functionalized monomer, the gels remained translucent, but at dye concentrations greater than 10⁻³ M, the aerogels became white and opaque.

2.7. Spectral Analysis. Steady-state emissions were recorded on a PTI spectrofluorimeter equipped with a model A-1010 arc lamp housing and a model 810/814 photomultiplier detector. Aged xerogels and aerogels were transferred to methacrylic cuvettes for spectral analysis. Aerogels were prepared in an autoclave (Thermo VG Scientific, E 3000 Super Critical Point Dryer). ¹H and ¹³C NMR were recorded on 300 and 400 MHz Varian spectrometers. N₂ sorption analysis of gel porosity was performed on a Quantachrome Autosorb-1 gas analyzer. BET analysis of aerogel samples indicated a pore size distribution in the mesoporous range, ca. 100 Å. No results could be obtained for xerogel samples, indicating that the average pore size fell below the measurable range of the instrument. Average pore sizes in the microporous range have been reported for TiO₂ xerogels.⁴⁶

SCHEME 1: Gelation of Titanate Derivatives (R = CH₂Pyr, CH₃, Ph)

3. Results and Discussion

The preparation of dye-modified aerogels and xerogels was easily achieved through the condensation illustrated in Scheme 1.²⁹ When 1-pyrenylmethyl-substituted titanate **1** was included within the reaction mixture, a covalently modified composite was attained. If, instead, pyrene itself were present in the gelation mixture, similar quantities of included dye could be trapped within the pores, as shown by concentration-dependent optical matching.

Various synthesis mixtures have been employed to control the local chemical environment within a gel matrix. Prepared samples can be categorized as eight distinct sample types prepared by different methods. These eight treatments are listed in Table 1. Specific treatments include the length of aging, the use of supercritical drying to form aerogels, and the displacement of one of the hydroxy functionalities in titanium alkoxide by 1-pyrenylmethyl, methyl, or phenyl groups. The last two sample types shown in Table 1 include unbound pyrene in place of the covalently bound species.

The representative fluorescence spectra of the resulting monoliths shown in Figure 1 were obtained for optically matched encapsulated (dashed line) and covalently bound 1-methylpyrene (solid line). The spectra exhibit vibronic bands in the 370–400 nm region that are characteristic of pyrene monomer emission³⁵ with somewhat higher emission intensity observed with the covalently bound chromophore. The relative intensities of the highest and lowest frequency bands, referred

TABLE 1: Relative Emission Intensities for Monomer and Excimer from Bound or Encapsulated Pyrenyl Groups Held within a TiO₂ Sol Gel Matrix^a

sample ^b	monomer $I_1/(I_1 + I_5)$ at 10 ⁻³ M	monomer $I_1/(I_1 + I_5)$ at 10 ⁻⁵ M	excimer $E/(E + I_e)$ at 10 ⁻³ M
1	0.57 ± 0.05	0.50 ± 0.02	0.40 ± 0.20
2	0.60 ± 0.03	0.55 ± 0.05	0.25 ± 0.15
3	0.62 ± 0.04	0.58 ± 0.02	0.35 ± 0.15
4	0.64 ± 0.01	0.62 ± 0.02	0.15 ± 0.05
5	0.60 ± 0.02	0.59 ± 0.04	0.04 ± 0.01
6	0.62 ± 0.01	0.57 ± 0.01	0.05 ± 0.01
7	0.58 ± 0.01	0.58 ± 0.03	0.10 ± 0.05
8	0.52 ± 0.01	0.48 ± 0.02	0.15 ± 0.02

^a Reproducibility was determined as the range of values from which was calculated the reported average value of three measurements on each of the separately prepared samples. ^b Sample 1 = xerogel from Ti(OCHMe₂)₄ doped with tethered pyrene **1** aged 5–6 weeks; sample 2 = xerogel from Ti(OCHMe₂)₄ doped with tethered pyrene **1** aged 3–4 weeks; sample 3 = aerogel from Ti(OCHMe₂)₄ doped with tethered pyrene **1**; sample 4 = xerogel from Ti(OCHMe₂)₄ doped with tethered pyrene **1** aged 5–6 weeks with 5% functionalized Ti(IV) monomer **2** in sol solution; sample 5 = xerogel from Ti(OCHMe₂)₄ doped with tethered pyrene **1** aged 3–4 weeks with 5% functionalized Ti(IV) monomer **2**; sample 6 = xerogel from Ti(OCHMe₂)₄ doped with tethered pyrene **1** aged 3–4 weeks with 1% of phenyl functionalized Ti(IV) monomer **3**; sample 7 = xerogel from Ti(OCHMe₂)₄ doped with encapsulated unbound pyrene aged 3–4 weeks; sample 8 = xerogel from Ti(OCHMe₂)₄ doped with encapsulated unbound pyrene aged 3–4 weeks with 1% of phenyl functionalized Ti(IV) monomer **3**.

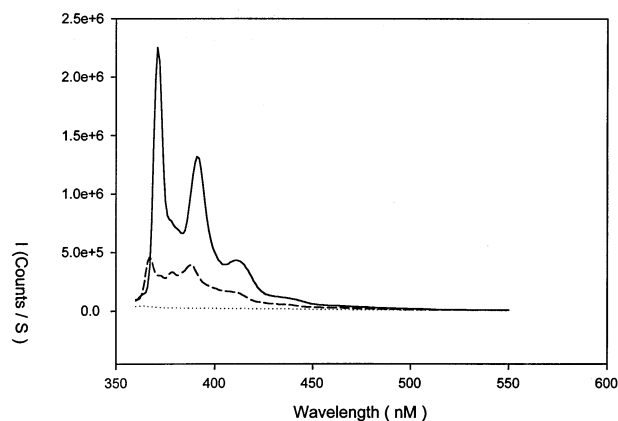


Figure 1. Steady-state fluorescence for covalently bound **1** (solid line) and occluded (dashed line) pyrene for titanate xerogel samples aged 3 weeks as monoliths prepared from 10⁻⁵ M sol solutions containing a 99:1 ratio of Ti(OCHMe₂)₄/CH₃Ti(OCHMe₂)₃. Excitation wavelength = 343 nm under air.

to as I_1 and I_5 , respectively, have been correlated to the local solvent polarities with a decreased $I_1/(I_1 + I_5)$ ratio indicating a reduction in local solvent polarity.^{35–38}

In Table 1, the relative intensities of I_1 ($I_1/(I_1 + I_5)$) and of the excimer emissions are recorded as a function of sample treatment. The most striking feature is the absence of major changes in intensity on gel type, except in the relative intensity of the observed excimer emission. The first and third columns describe monomer and excimer emission from gels at a dye concentration of 10⁻³ M of either the tethered or unbound pyrene species in the sol solution, while the second column describes monomer emission from a less highly doped gel (10⁻⁵ M). Type 1 and 2 gels (aged xerogel titanates) show strong monomer emission, indicating isolation of the pyrene groups within the polar titanate matrix. The relative I_1 intensity among these xerogels was slightly lower, on average, for less compact gels, types 2 and 3. These samples also showed weaker emission

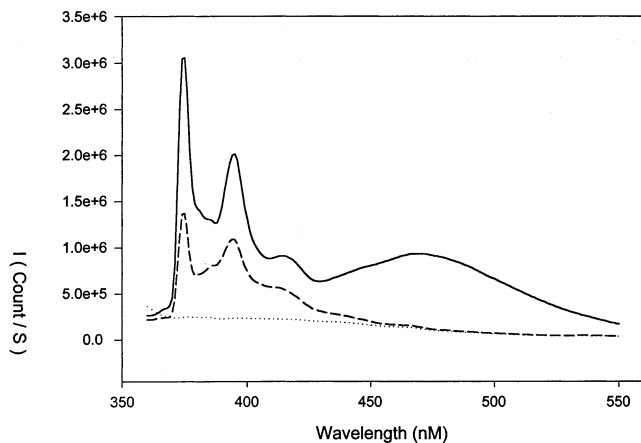


Figure 2. Steady-state fluorescence for xerogels of covalently bound pyrene **1** aged 5 weeks as titanate monoliths aged 3 weeks. Initial chromophore concentration in the sol = 10^{-5} M (dashed line) and 10^{-3} M (solid line). Excitation wavelength = 343 nm under air.

than did the samples prepared through longer aging of xerogels or by preparation of the aerogel. Type 4 gels, in which methyl groups had replaced a portion of the bridging hydroxy groups, exhibited the highest relative intensity for I_1 , consistent with a lower local polarity for the entrapped dye.

At lower concentrations of the tethered pyrene (column 2), the type 1 gels exhibited lower relative intensity of I_1 , except for type 7 gels, which contained unbound pyrene. These samples exhibited, however, a higher I_1 intensity at lower chromophore concentration. These trends suggest that equilibration of pyrene groups into hydrophobic pockets induces a reduction in the relative I_1 intensity by favoring arene–arene interaction, likely through π stacking.⁴⁶ Aging permitted sufficient migration of the hydrophobic dye to the more favorable emission site, as can be seen in the small intensity changes from sample 4 to sample 5. Somewhat less efficient emission is observed when the pyrenyl probe is trapped but not covalently bound, as in gels 7 and 8. With a less polar environment, the enthalpic gain from π stacking within a pyrene aggregate is minimized. A similar shift was also seen in sample 6.

The spectral shifts in Figure 2 reflect the effect of pyrene concentration on the magnitude of the observed excimer signal. Strong excimer signals (ca. 470 nm) are observed for highly polar aerogels and xerogels (types 1–3) when the concentration of the bound pyrene **1** is 10^{-3} M (Table 1, column 3). Type 1 gels, which are the most compact, exhibited the highest relative excimer intensity. Less compact gels, like type 2 and type 3 gels, exhibited a somewhat weaker excimer signal. This trend is consistent with results obtained for pyrene adsorbed on preformed silica, for which the intensity of the excimer signal was smaller for large pore silicas.^{35,40,47,48} The strong excimer signal exhibited by type 1 gels is also consistent with the observed reduction in the relative I_1 intensity.

In a study of the kinetics of gelation in silica matrices, Avnir et al. found that the intensity of the excimer signal reached a maximum value as condensation proceeded and then gradually declined within 3–6 weeks.^{35,36} The gradual decline was attributed to the isolation of individual molecules within the porous structure. The difference between this earlier study and our current analysis may be attributed to fundamental differences in the surface structures and porosity of TiO₂ and silica xerogels, especially when an organic substituent is bound to an included titanium atom.

The inclusion of methyl and phenyl functional groups within the matrix (gels 4–6) obstructed the formation of excimers,

presumably by providing hydrophobic pockets that could receive the pyrenyl chromophore and compete with excimer emission. The same effect was observed, although somewhat less pronounced, in monoliths doped with unbound pyrene, gels 7 and 8.

4. Conclusions

Steady-state fluorescence was used successfully to probe the interaction between a substituted pyrene either covalently bound as a 1-pyrenylmethyl group or noncovalently trapped as neutral 1-methylpyrene within a TiO₂ gel monolith. The relative intensities of monomer and excimer emissions of the included pyrene were used to characterize the polarity of the local environment encountered in the gel interior. Reduction in the relative intensity of I_1 as a function of pyrene concentration and local polarity suggests that aggregation of nearby pyrene groups can readily take place. The presence of a matrix-induced methyl or phenyl group was observed in either the tethered or unbound pyrenes to inhibit pyrene–pyrene association through π stacking. Changes observed in the relative intensity of the excimer emission suggest that the phenyl or methyl groups within the matrix reduce the driving force for association of neighboring tethered pyrenes. Excimer emission was less efficient in less compact gel samples, specifically in incompletely aged aerogels and xerogels and in trapped (noncovalently bound) clathrate sites.

Acknowledgment. We gratefully acknowledge support of the work by the National Science Foundation (Grants CHE-9901213 and CHE-9876674). The authors also thank Professor Maryanne Collinson of Kansas State University, who performed the N₂ sorption analysis.

References and Notes

- Boilot, J.-P.; Biteau, J.; Brun, A.; Chaput, F.; De Morais, T. D.; Darracq, B.; Gacoin, T.; Lahlil, K.; Lehn, J.-M.; Levy, Y.; Malier, L.; Tsvigoulis, C.-M. *Mater. Res. Soc. Symp. Proc.* **1998**, *519*, 227.
- Fujii, T.; Tanaka, N.; Tai, H.; Obara, S.; Ellis, A. B. *Bull. Chem. Soc. Jpn.* **2000**, *73*, 809.
- Lal, M.; Levy, L.; Kim, K. S.; He, G. S.; Wang, X.; Min, Y. H.; Pakatchi, S.; Prasad, P. N. *Chem. Mater.* **2000**, *12*, 2632.
- Huber, R.; Spörlein, S.; Moser, J. E.; Grätzel, M.; Wachtveitl, J. *J. Phys. Chem. B* **2000**, *104*, 8995.
- Zheng, J.-P.; Gu, M.-Y.; Jin, Y.-P.; Jin, Y.-P.; Wang, H.-H.; Zu, P.-F.; Tao, P.; He, J.-B. *Mater. Sci. Eng.* **2001**, *B87*, 197.
- Zhang, X.; Du, S.; Chen, Y.; Zhang, L.; Cao, Y.; Chai, X.; Bai, Y.; Liangzhi, X.; Li, T. *Thin Solid Films* **1998**, *327–329*, 563.
- Ivanda, M.; Musić, S.; Gotis, M. *J. Mol. Struct.* **1999**, *480–481*, 645.
- Znaida, L.; Séraphimova, R.; Bocquet, J. F.; Colbeau-Justin, C.; Pommier, C. *Mater. Res. Bull.* **2001**, *36*, 811.
- Mao, H.; Deng, J.; Li, H.; Shen, Y.; Lu, Z.; Xu, H. *J. Photochem. Photobiol., A: Chem.* **1998**, *114*, 209.
- Yang, J. H.; Chen, Y. M.; Ren, Y. L.; Bai, Y. B.; Wu, Y.; Jang, Y. S.; Su, Z. M.; Yang, W. S.; Wang, Y. Q.; Zao, B.; Li, T. *J. Photochem. Photobiol., A: Chem.* **2000**, *134*, 1.
- Osora, H.; Li, W.; Otero, L.; Fox, M. A. *J. Photochem. Photobiol., B: Biol.* **1998**, *134*, 232.
- Garzella, C.; Comini, E.; Tempesti, E.; Frigeri, C.; Sberveglieri, S. *Sens. Actuators, B* **2000**, *68*, 189.
- (a) Fox, M. A. *Trace Met. Environ.* **1993**, *3*, 163. (b) Fox, M. A. *Acc. Chem. Res.* **1983**, *16*, 314.
- Fox, M. A.; Dulay, M. T. *Chem. Rev.* **1993**, *93*, 341.
- Torimoto, T.; Fox, R. J., III; Fox, M. A. *J. Electrochem. Soc.* **1996**, *143*, 3712.
- Yamashita, H.; Kawasaki, S.; Ichihashi, Y.; Harada, M.; Takeuchi, M.; Anpo, M.; Stewart, G.; Fox, M. A.; Louis, C.; Che, M. *J. Phys. Chem. B* **1998**, *102*, 5870.
- Yamashita, H.; Ichihashi, Y.; Harada, M.; Stewart, G.; Fox, M. A.; Anpo, M. *J. Catal.* **1996**, *158*, 97.
- Al-Ekabi, H.; Serpone, N.; Pelizzetti, E.; Minero, C.; Fox, M. A.; Draper, R. B. *Langmuir* **1989**, *5*, 250.

- (19) Grätzel, M. *Chem. Rev.* **1994**, *94*, 316.
- (20) Bonhôte, P. E.; Moser, J.-E.; Humphry-Baker, R.; Vlachopoulos, N.; Zakeeruddin, S. M.; Walder, L.; Grätzel, M. *J. Am. Chem. Soc.* **1999**, *121* (1), 1324.
- (21) Bonhôte, P. E.; Gogniat, E.; Tingry, S.; Barbé, N.; Vlachopoulos, N.; Lenzmann, F.; Comte, P.; Grätzel, M. *J. Am. Chem. Soc.* **1980**, *102* (2), 1498.
- (22) Nazeeruddin, M. K.; Péchy, P.; Renouard, T.; Zakeeruddin, S. M.; Humphry-Baker, R.; Comte, P.; Liska, P.; Cevey, L.; Costa, E.; Shklover, V.; Spiccia, L.; Deacon, G. B.; Bignozzi, C. A.; Grätzel, M. *J. Am. Chem. Soc.* **2001**, *123*, 1613.
- (23) Hagfeldt, A.; Grätzel, M. *Chem. Rev.* **1995**, *95*, 49.
- (24) Brinker, J.; Scherer, G. *Sol-Gel Science*; Academic Press: New York, 1989.
- (25) Collinson, M. M. *Crit. Rev. Anal. Chem.* **1999**, *29*, 289.
- (26) Collinson, M. M. *Trends Anal. Chem.* **2002**, *21*, 30.
- (27) Yoldas, B. E. *J. Mater. Sci.* **1986**, *21*, 1087.
- (28) Swider, K. E.; Merzbacher, C. I.; Hagans, P. L.; Rolison, D. R. *Chem. Mater.* **1997**, *9*, 1248.
- (29) (a) Chambers, R. C.; Haruvy, Y.; Fox, M. A. *Chem. Mater.* **1994**, *6*, 1351. (b) Hiromi Yamashita, H.; Kawasaki, S.; Ichihashi, Y.; Harada, M.; Takeuchi, M.; Anpo, M.; Stewart, G.; Fox, M. A.; Louis, C.; Che, M. *J. Phys. Chem. B* **1998**, *102*, 5870.
- (30) Löbmann, P.; Glaubitt, W.; Geis, S.; Fricke, J. *J. Non-Cryst. Solids* **1998**, *225*, 130.
- (31) Lan, E. H.; Dave, B. C.; Fukuto, J. M.; Dunn, B.; Zink, J. I.; Valentine, J. S. *J. Mater. Chem.* **1999**, *9*, 45.
- (32) Correia, S. M. G.; Bermudez, V. D. Z.; Ferreira, R. A. S.; Carlos, L. D.; Silva, M. M.; Barros, S.; Smith, M. J. *Ionics* **2002**, *8*, 73.
- (33) Franville, A.-C.; Zambon, D.; Mahiou, R.; Troin, Y. *Chem. Mater.* **2000**, *12*, 428.
- (34) Joshi, M. P.; DeLeon, R. L.; Prasad, P. N.; Garvey, J. F. *J. Appl. Phys.* **1999**, *85*, 3928.
- (35) Kaufman, V. R.; Avnir, D. *Langmuir* **1986**, *2*, 717.
- (36) Birenbaum, H.; Avnir, D.; Ottolenghi, M. *Langmuir* **1989**, *5*, 48.
- (37) (a) Ruetten, S. A.; Thomas, J. K. *J. Phys. Chem. B* **1999**, *103*, 1278. (b) Ruetten, S. A.; Thomas, J. K. *Langmuir* **2000**, *16*, 234.
- (38) Chambers, R. C.; Jones, W. E., Jr.; Havy, Y.; Webber, S. E.; Fox, M. A. *Chem. Mater.* **1993**, *5*, 1481.
- (39) Ilharco, L. M.; Santos, A. M.; Silva, M. J.; Martinho, J. M. G. *Langmuir* **1995**, *11*, 2419.
- (40) Lacombe, S.; Cardy, H.; Soggiu, N.; Blanc, S.; Habib-Jiwan, J. L.; Soumillion, J. P. *Microporous Mesoporous Mater.* **2001**, *46*, 311.
- (41) Ulman, A. *Chem. Rev.* **1996**, *96*, 1533.
- (42) Rausch, M. D.; Gordon, H. B. *J. Organomet. Chem.* **1974**, *74*, 85.
- (43) Clauss, K. *Liebigs Ann. Chem.* **1968**, *711*, 19.
- (44) Dagan, G.; Tomkiewicz, M. *J. Phys. Chem.* **1993**, *97*, 12651.
- (45) Campbell, L. K.; Na, B. K.; Ko, E. I.; *Chem. Mater.* **1992**, *4*, 1329.
- (46) Dagan, G.; Tomkiewicz, M. *J. Non-Cryst. Solids* **1994**, *175*, 294.
- (47) Hirakawa, K.; Segawa, H. *J. Photochem. Photobiol., A: Chem.* **1999**, *123*, 67.
- (48) Xu, Q.; Anderson, M. A. *J. Am. Ceram. Soc.* **1994**, *77*, 1939.